JACS
JOURNAL OF THE AMERICAN CHEMICAL SOCIETY
Communication
pubs.acs.org/JACS

Equatorially Coordinated Lanthanide Single Ion Magnets

Peng Zhang,[†,‡] Li Zhang,[†,‡] Chao Wang,[†] Shufang Xue,[†,‡] Shuang-Yan Lin,[†,‡] and Jinkui Tang*[,†]

[†]State Key Laboratory of Rare Earth Resource Utilization, Changchun Institute of Applied Chemistry, Chinese Academy of Sciences, Changchun 130022, P. R. China

[‡]University of Chinese Academy of Sciences, Beijing, 100049, P. R. China

Supporting Information

ABSTRACT: The magnetic relaxation dynamics of low-coordinate Dy^{III} and Er^{III} complexes, namely three-coordinate ones with an equatorially coordinated triangle geometry and five-coordinate ones with a trigonal bipyramidal geometry, have been exploited for the first time. The three-coordinate Er-based complex is the first equatorially coordinated mononuclear Er-based single-molecule magnet (SMM) corroborating that simple models can effectively direct the design of target SMMs incorporating 4f-elements.

An area of particular concern in the research of single molecule magnets (SMMs)[1] in recent years is the investigation of systems with only one spin carrier within a molecule.[2−5] Remarkably, the record value of effective barrier in SMM field is still kept to date by a heteroleptic bis(phthalocyaninate) SMM, $[Tb^{III}(Pc)(Pc')]$ (U_{eff} = 652 cm^{-1}/939 K).[6] Here the high barriers and blocking temperatures in bis(phthalocyaninate) lanthanide complexes can be directly related to the crystal field with highly axial symmetry (C_4, even S_8 axis) created by the surrounding ligands.[7−9] Therefore, how to enhance the axial anisotropy around lanthanide ion has been an important subject for the improvement of SMM properties.[10−15] In 2011, Long et al. put forward a simple but amenable model for predicting the ligand architectures that will generate strong magnetic anisotropy for a variety of 4f-element ions based on their basic overall shape of free-ion electron density.[16,17] Two representative examples are the Kramers ions Dy^{III} ($^6H_{15/2}$) and Er^{III} ($^4I_{15/2}$) with oblate and prolate-shaped electron densities, respectively.[18] Herein, to give a highly anisotropic ground state with a large $\pm m_J$, Dy^{III} ion should be located in sandwich-type ligand geometry, maximizing the anisotropy of an oblate ion. Inversely, an equatorially coordinated geometry is predicted to be preferable for Er^{III} ion. However, such a coordination geometry is difficult to be constructed because of the high coordination numbers of lanthanide ions,[19] and thus mononuclear Er-based SMM with a perfect equatorially coordinate geometry has been lacking so far. Actually Er-containing SMMs are very rare, and a few examples exhibiting only equatorially coordinated ligands or equatorial field have been reported.[2,20−23] Nevertheless, in an intermetallic compound $SmCo_5$, the Sm^{III} ions with prolate electron densities are coupled with six equatorially coordinated cobalt atoms with the delocalized electrons, providing the high magnetic anisotropy and thus generating one of the strongest magnets known.[16] Indeed, both the heteroleptic ErCp*(COT) and homoleptic $[Er(COT)_2]^-$ have recently been proven to be more efficient SMMs than their Dy^{III} congeners.[2,22,24] In spite of the seeming sandwich-type structure, the *ab initio* calculations for $[Dy(COT)_2]^-$ indicated that the equatorial component of the ligand field is stronger than the axial one.[25] Therefore, the interest in an equatorially coordinated molecular species is driven greatly by the potential of developing SMMs with high barriers and blocking temperature.

Given that low-coordinate complexes can provide more opportunities to get the highly axial equatorially coordinate geometry such as triangle and square, we determined to explore low-coordinate lanthanide complexes in pursuit of a mononuclear SMM model compound with equatorially coordinated geometry. In fact, such low-coordinate lanthanide complexes have been extensively investigated in organometallic chemistry,[19,26] however their low-temperature magnetic dynamics is substantially unexplored. Herein, two classes of lanthanide compounds with low-coordination numbers were chosen by us for their initial magnetic studies. One class is the three-coordinate lanthanide complexes, $Ln[N(SiMe_3)_2]_3$ (Ln = Dy^{III}, **1a** and Er^{III}, **1b**), showing an equatorially coordinated triangle geometry with a perfect C_3 axis.[27−30] Amazingly, the Er complex, **1b**, behaves as the first equatorially coordinated mononuclear Er-based SMM (*vide infra*) that fulfills the simple model developed by Long et al. In fact, the C_3 symmetry mononuclear Dy or Er SMMs with a high coordinate number, such as six or seven-coordinate, have been explored before, but all show the fast zero-field quantum tunneling of magnetization (QTM) and thus a field-induced SMM behavior due to the large mixing of different m_J states.[31−33] Here on lowing the coordinate number, the crystal field only in equatorial positions around the Er ion extremely enhances the unaxial anisotropy and thus efficiently suppresses the zero-field QTM in spite of 'nonaxial' parameters in C_3 crystal field analysis. The other class is the five-coordinate complexes, $Ln(NHPh^iPr_2)_3(THF)_2$ (Ln = Dy^{III}, **2a** and Er^{III}, **2b**), with a trigonal bipyramidal geometry.[34] Both of them (**2a** and **2b**) exhibit slow magnetic relaxation in a zero/nonzero dc applied field, which can be elucidated through the comparison of electronic structures between **1** and **2**.

The synthesis of $Ln[N(SiMe_3)_2]_3$ (**1**) was originally pioneered in 1972 by D. C. Bradley.[27] Subsequently, the complexes with different lanthanide ions attracted considerable attention as special examples for the low coordination number of lanthanide compounds and as starting compounds for

Received: January 28, 2014
Published: March 13, 2014

dx.doi.org/10.1021/ja500793x | J. Am. Chem. Soc. 2014, 136, 4484−4487

preparing the tetrahydrofuran-free molecular compounds of lanthanides ions (amide route).[26,28] Single-crystal X-ray studies revealed that compound **1** crystallizes in the trigonal space group *P*-31*c* with high symmetry (Table S1 and Figure S1). The molecular structure in Figure 1a demonstrates that the

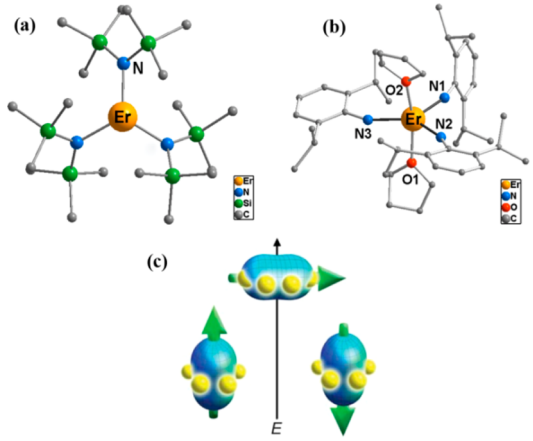

Figure 1. Molecular structures of compounds **1** (a) and **2** (b). The H atoms have been omitted for clarity. (c) Depiction of low- and high-energy configuration of the f-orbital electron density with respect to an equatorial crystal field for a 4f ion with prolate electron density. Reproduced from ref 16 with permission of The Royal Society of Chemistry.

central ion is coordinated by three N atoms in the shape of a flat trigonal pyramid and disordered over two positions above and below the N_3 plane, leading to an effective ligand field of C_{3v} symmetry. In terms of most mononuclear lanthanide SMMs, the axial symmetry is only limited to the coordination geometry of central ion, but not for the whole molecule. It is noteworthy that such a high axial symmetry in the whole molecule provides us a great opportunity for exploring its effects on QTM and SMM behavior. Compound **2** was synthesized by adopting the procedure given by W. J. Evans in 1996.[34] As shown in Figure 1b, the metal center is approximately trigonal bipyramid (Table S2) with the three large electronegative amido ligands in the equatorial positions and two axially coordinating THF molecules. Thus the negative charges are still concentrated in the equatorial positions of metal center, and compound **2b** shows an average Er^{III}–N distance of 2.1871 Å close to 2.1914 Å in **1b**. In contrast to **1**, the coordination of two THF molecules breaks the equatorially coordinating geometry, enabling us to study its effects on SMM behavior of Dy^{III} and Er^{III} complexes, respectively. In a packing diagram for compounds **1** and **2**, the shortest intermolecular Dy···Dy distances are more than 9 Å, suggesting the negligible intermolecular magnetic interactions.

Before discussing the magnetic properties, the electronic structures of compounds **1a** and **1b** were provided because the crystal field splitting pattern has been stimulated through applying the crystal field Hamiltonians for C_{3v} symmetry by H.-D. Amberger in 1998 and 2008.[28,29] As shown in Figure 2, the doublet ground states are distinct for Dy (**1a**) and Er (**1b**) compounds due to their opposite shape of free-ion electron density. Clearly, the Dy compound (**1a**) shows ground states with the smallest $m_J = \pm 1/2$ component, and the m_J states are ordered from lowest to highest, behaving as the hard-axis or easy-plane properties. On the contrary, the easy-axis property is realized in the Er compound (**1b**) showing the highest ground

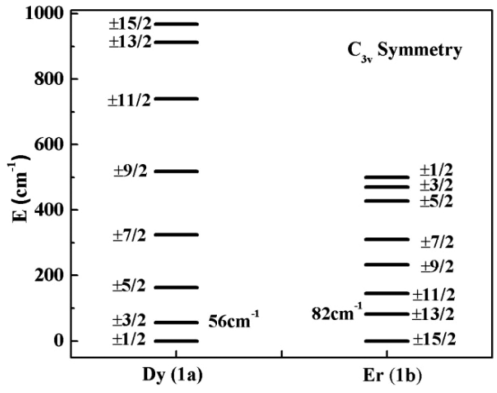

Figure 2. Energy and m_J values of the sublevels of the ground multiplets of $Ln[N(SiMe_3)_2]_3$ (Ln = Dy^{III} and Er^{III}).[28,29]

states $m_J = \pm 15/2$ and the order of m_J states from highest to lowest. The completely opposite results for Dy and Er ions are consistent with the prediction of the model from Long et al. For Er ion, such an equatorially coordinating geometry minimizes charge contact with the axially located f-element electron density, which stabilizes high magnitude m_J as ground state, as shown in Figure 1c.[16]

The variable-temperature dc magnetic susceptibility data for **1** and **2** collected under a 1 kOe applied field reveal the reasonable room-temperature $\chi_M T$ values of 13.95 (**1a**), 11.16 (**1b**), 14.56 (**2a**), and 11.39 (**2b**) cm^3 K mol^{-1} (Figure 3). As

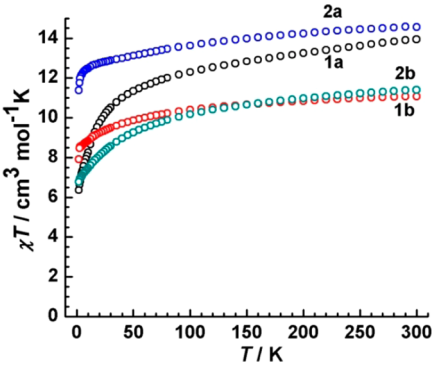

Figure 3. Susceptibility temperature product χT as a function of temperature recorded on samples of **1** and **2** in an applied field of 1 kOe.

the temperature is lowered, $\chi_M T$ product displays a slight decrease for compounds **2a** and **2b** as a result of the depopulation of the Stark sublevels and/or significant magnetic anisotropy present in lanthanide systems. In contrast, compound **1a** demonstrates an obvious decrease to 6.35 cm^3 K mol^{-1} at 2 K, which can be ascribed to the ground states with smallest m_J component ($\pm 1/2$).

Ac susceptibility measurements reveal that complex **1a** does not exhibit any out-of phase (χ'') ac signals typical of an SMM under zero applied dc field, and the application of a dc field resulted in very weak ac signals with no frequency-dependent peaks in plots of χ'' vs ν (Figure S3). In contrast, SMM behavior is observed for the Er analogue **1b** as evidenced by well resolved out-of-phase ac susceptibility maxima that vary with frequency (Figure 4 top and S4). Here the maxima in χ'' vs ν plots indicates the "freezing" of the spins by the anisotropy barriers at low-temperature region. The distinct relaxation

dx.doi.org/10.1021/ja500793x | J. Am. Chem. Soc. 2014, 136, 4484−4487

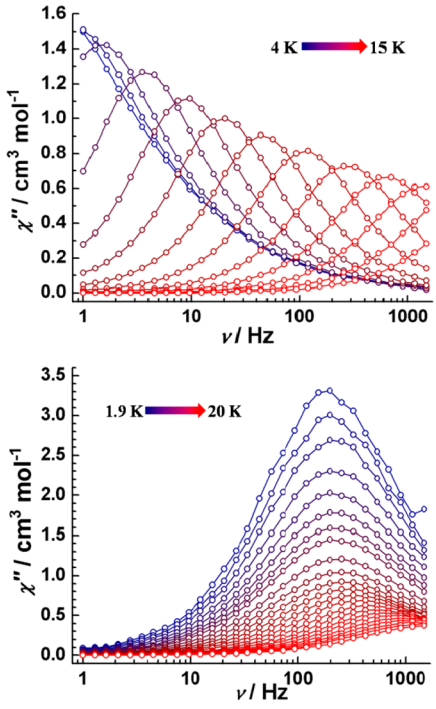

Figure 4. Temperature dependence of χ'' for samples **1b** (top) and **2a** (bottom) under a zero applied dc field, with an ac field of 3 Oe.

behavior between **1a** and **1b** is a consequence of the completely different electronic structures, as evidenced in Figure 2, of Dy and Er analogue under the special equatorially coordinating crystal field. The ground states with very small quantum numbers, $m_J = \pm 1/2$, of Dy ions is unfavorable for strong single-molecule magnetism, well in agreement with the results of ac susceptibility measurements (only a weak field-induced relaxation behavior). Fitting the Cole−Cole plots to the generalized Debye functions to determine relaxation times gave small distributions ($0.01 < \alpha < 0.17$ at temperature between 6 and 14 K, Figure S6) for **1b**.

By contrast, ac magnetic susceptibility measurements were also performed on microcrystalline samples of compounds **2a** and **2b**. For Dy-based compound **2a**, the slow relaxation behavior of magnetization can be observed at temperature as high as 40 K, but the rapidly increasing out-of-phase (χ'') ac magnetic susceptibility below 10 K in χ'' vs T plots is indicative of a strong tunneling relaxation between the ground Kramers doublet for this compound (Figures 4 bottom and S7 and S9). In contrast to the absence of SMM behavior in compound **1a**, compound **2a** shows clear zero-field SMM behavior in spite of the fast tunneling relaxation at low temperature. Indeed, the coordination of two THF molecules above and below equatorial plane breaks the equatorially coordinating crystal field around Dy ions, which shifts one state with a high m_J quantum number to its ground state and thus leads to the large magnetic moment of ground states. It seems that for Dy-based compounds low-symmetry crystal field components could promote the presence of SMM behavior for some specific symmetries or ligand surroundings. This also provides a reasonable explanation why some mononuclear lanthanide compounds with low-symmetry behave as effective SMMs.[35−37] The Cole−Cole plots can be fitted to the generalized Debye model with α parameters below 0.25 between 1.9 and 20 K, indicating a very narrow distribution of relaxation times (Figure S10). For Er-based compound **2b**, the SMM behavior was also observed through the application of a static field, as indicated by the appearance of peaks in the out-of-phase (χ'') component in χ'' vs ν plots (Figures S11 and S12). The results can be rationalized in terms of the crystal structure of compound **2b**, where the negative charges are still concentrated in the equatorial positions of Er center. However, the increasing transverse components of anisotropy as a consequence of the coordination of THF molecules lead to the fast quantum tunneling and the subsequent disappearance of SMM behavior under zero applied field.

The magnetization relaxation time (τ) is extracted from the frequency dependence measurements and an Arrhenius fit to the data gives the effective relaxation barriers of compounds **1b**, **2a**, and **2b**. For **1b**, τ has not reached the pure quantum regime yet but nevertheless shows a weak deviation from the expected thermally activated behavior (Figure 5 top), which should be

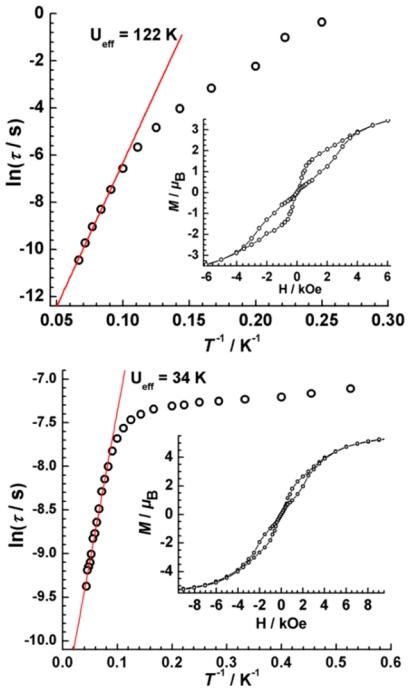

Figure 5. Magnetization relaxation time constant as $\ln(\tau)$ vs T^{-1} for **1b** (top) and **2a** (bottom) in a zero static field from best fit to the Arrhenius law of the thermally activated regime (solid line). Inset: Molar magnetization at 1.9 K.

due to the weak quantum tunneling of magnetization induced by the presence of rhombic anisotropy component in C_{3v} symmetry or other relaxation processes (Raman and direct). At a high-temperature regime, the effective barrier (U_{eff}) is 122 K (85 cm^{-1}, $\tau_0 = 9.33 \times 10^{-9}$ s), which is consistent with the energy separation (82 cm^{-1}) between the first excited states and the ground states determined by the simulation of crystal field splitting pattern (Figure 2), suggesting a thermally activated tunneling mechanism or an Orbach process via the first excited states.[38] For Dy-based compound **2a**, a crossover from a thermally activated to a temperature-independent regime in relaxation is clearly observed (Figure 5 bottom). At high temperature ($T > 11$ K), the relaxation follows an Arrhenius-like behavior, affording a barrier $U_{eff} = 34$ K with $\tau_0 = 2.07 \times 10^{-5}$ s. In addition, an effective barrier of 25 K (Figure S13) is given through an Arrhenius fit with $\tau_0 = 6.44 \times 10^{-8}$ s

dx.doi.org/10.1021/ja500793x | J. Am. Chem. Soc. 2014, 136, 4484−4487

for compound **2b** under an optimum field of 400 Oe (Figure S12). The barriers of compounds **2a** and **2b** seem to be small compared with that of **1b** as a result of the fast quantum tunneling. Obviously, butterfly-shaped magnetic hysteresis in **1b** and **2a** are observed using the sweep rate accessible with a conventional magnetometer (Figure 5 inset) at 1.9 K.

In conclusion, we have provided the first equatorially coordinated mononuclear Er-based molecular species behaving as an effective SMM following the useful model developed by Long et al. The three-coordinate lanthanide compounds demonstrate an equatorially coordinating crystal field with a perfect C_3 axis around lanthanide ions, which drives Er compound **1b** behaving as an strong SMM with effective suppression of QTM, while Dy compound does not show any SMM behavior. The crystal field calculations for Er ion are also compatible with the relaxation behavior *via* the first excited states. In contrast, the five-coordinate complexes of both Dy and Er ions display slow relaxation behavior of magnetization despite the fast QTM at low temperature, which should benefit from the modification of equatorially coordinating geometries. This work offers a means to exploit single ion effects of lanthanide possessing perfect axial symmetry in order to facilitate magnetic relaxation climbing up to a higher energy levels and demonstrates that low-coordinate lanthanide complexes could potentially serve as an important avenue to improve SMM properties. The results herein describe further proof that the use of a simple model without complicated calculations or comprehensive empirical characterization of the crystal field can effectively guide the design of new SMMs, which is definitely beneficial to exploratory research.

■ ASSOCIATED CONTENT

Supporting Information

Experimental procedure; physical measurements; crystallography; structural and magnetic tables and figures. This material is available free of charge via the Internet at http://pubs.acs.org.

■ AUTHOR INFORMATION

Corresponding Author

tang@ciac.ac.cn

Notes

The authors declare no competing financial interest.

■ ACKNOWLEDGMENTS

This work was supported by the National Natural Science Foundation of China (21371166, 21221061 and 21331003).

■ REFERENCES

(1) Christou, G.; Gatteschi, D.; Hendrickson, D. N.; Sessoli, R. *MRS Bull.* **2000**, *25*, 66.

(2) Jiang, S.-D.; Wang, B.-W.; Sun, H.-L.; Wang, Z.-M.; Gao, S. *J. Am. Chem. Soc.* **2011**, *133*, 4730.

(3) Zhang, P.; Guo, Y.-N.; Tang, J. *Coord. Chem. Rev.* **2013**, *257*, 1728.

(4) Jiang, S. D.; Wang, B. W.; Su, G.; Wang, Z. M.; Gao, S. *Angew. Chem., Int. Ed.* **2010**, 7448.

(5) Jeletic, M.; Lin, P.-H.; Le Roy, J. J.; Korobkov, I.; Gorelsky, S. I.; Murugesu, M. *J. Am. Chem. Soc.* **2011**, *133*, 19286.

(6) Ganivet, C. R.; Ballesteros, B.; de la Torre, G.; Clemente-Juan, J. M.; Coronado, E.; Torres, T. *Chem.—Eur. J.* **2013**, *19*, 1457.

(7) Ishikawa, N.; Sugita, M.; Ishikawa, T.; Koshihara, S.-y.; Kaizu, Y. *J. Am. Chem. Soc.* **2003**, *125*, 8694.

(8) Ishikawa, N.; Sugita, M.; Ishikawa, T.; Koshihara, S.; Kaizu, Y. *J. Phys. Chem. B* **2004**, *108*, 11265.

(9) Ishikawa, N.; Sugita, M.; Wernsdorfer, W. *Angew. Chem., Int. Ed.* **2005**, *44*, 2931.

(10) Boulon, M.-E.; Cucinotta, G.; Luzon, J.; Degl'Innocenti, C.; Perfetti, M.; Bernot, K.; Calvez, G.; Caneschi, A.; Sessoli, R. *Angew. Chem., Int. Ed.* **2013**, *52*, 350.

(11) Car, P.-E.; Perfetti, M.; Mannini, M.; Favre, A.; Caneschi, A.; Sessoli, R. *Chem. Commun.* **2011**, *47*, 3751.

(12) Layfield, R. A. *Organometallics* **2014**, *33*, 1084.

(13) Rinehart, J. D.; Fang, M.; Evans, W. J.; Long, J. R. *Nat. Chem.* **2011**, *3*, 538.

(14) Rinehart, J. D.; Fang, M.; Evans, W. J.; Long, J. R. *J. Am. Chem. Soc.* **2011**, *133*, 14236.

(15) Demir, S.; Zadrozny, J. M.; Nippe, M.; Long, J. R. *J. Am. Chem. Soc.* **2012**, *134*, 18546.

(16) Rinehart, J. D.; Long, J. R. *Chem. Sci.* **2011**, *2*, 2078.

(17) Kajiwara, T.; Nakano, M.; Takahashi, K.; Takaishi, S.; Yamashita, M. *Chem.—Eur. J.* **2011**, *17*, 196.

(18) Skomski, R. *Simple Models of Magnetism*; Oxford University Press: New York, 2008.

(19) Huang, C., *Rare Earth Coordination Chemistry: Fundamentals and Applications*; John Wiley & Sons (Asia) Pte Ltd: Singapore, 2010.

(20) Yamashita, A.; Watanabe, A.; Akine, S.; Nabeshima, T.; Nakano, M.; Yamamura, T.; Kajiwara, T. *Angew. Chem., Int. Ed.* **2011**, *50*, 4016.

(21) AlDamen, M. A.; Clemente-Juan, J. M.; Coronado, E.; Martí-Gastaldo, C.; Gaita-Ariño, A. *J. Am. Chem. Soc.* **2008**, *130*, 8874.

(22) Meihaus, K. R.; Long, J. R. *J. Am. Chem. Soc.* **2013**, *135*, 17952.

(23) Palacios, M. A.; Titos-Padilla, S.; Ruiz, J.; Herrera, J. M.; Pope, S. J. A.; Brechin, E. K.; Colacio, E. *Inorg. Chem.* **2014**, *53*, 1465.

(24) Le Roy, J. J.; Korobkov, I.; Murugesu, M. *Chem. Commun.* **2014**, *50*, 1602.

(25) Le Roy, J. J.; Jeletic, M.; Gorelsky, S. I.; Korobkov, I.; Ungur, L.; Chibotaru, L. F.; Murugesu, M. *J. Am. Chem. Soc.* **2013**, *135*, 3502.

(26) Lappert, M.; Protchenko, A.; Power, P.; Seeber, A. *Metal Amide Chemistry*; John Wiley & Sons Ltd: United Kingdom, 2009.

(27) Bradley, D. C.; Ghotra, J. S.; Hart, F. A. *J. Chem. Soc., Chem. Commun.* **1972**, 349.

(28) Jank, S.; Amberger, H. D.; Edelstein, N. M. *Spectrochim. Acta Part A* **1998**, *54*, 1645.

(29) Jank, S.; Reddmann, H.; Amberger, H. D. *Inorg. Chim. Acta* **2008**, *361*, 2154.

(30) Herrmann, W. A.; Anwander, R.; Munck, F. C.; Scherer, W.; Dufaud, V.; Huber, N. W.; Artus, G. R. J. *Z. Naturforsch.* **1994**, *B49*, 1789.

(31) Meihaus, K. R.; Rinehart, J. D.; Long, J. R. *Inorg. Chem.* **2011**, *50*, 8484.

(32) Pedersen, K. S.; Ungur, L.; Sigrist, M.; Sundt, A.; Schau-Magnussen, M.; Vieru, V.; Mutka, H.; Rols, S.; Weihe, H.; Waldmann, O.; Chibotaru, L. F.; Bendix, J.; Dreiser, J. *Chem. Sci.* **2014**, *5*, 1650.

(33) Lucaccini, E.; Sorace, L.; Perfetti, M.; Costes, J.-P.; Sessoli, R. *Chem. Commun.* **2014**, *50*, 1648.

(34) Evans, W. J.; Ansari, M. A.; Ziller, J. W.; Khan, S. I. *Inorg. Chem.* **1996**, *35*, 5435.

(35) Watanabe, A.; Yamashita, A.; Nakano, M.; Yamamura, T.; Kajiwara, T. *Chem.—Eur. J.* **2011**, *17*, 7428.

(36) Feltham, H. L. C.; Lan, Y.; Klöwer, F.; Ungur, L.; Chibotaru, L. F.; Powell, A. K.; Brooker, S. *Chem.—Eur. J.* **2011**, *17*, 4362.

(37) Woodruff, D. N.; Winpenny, R. E. P.; Layfield, R. A. *Chem. Rev.* **2013**, *113*, 5110.

(38) Blagg, R. J.; Ungur, L.; Tuna, F.; Speak, J.; Comar, P.; Collison, D.; Wernsdorfer, W.; McInnes, E. J. L.; Chibotaru, L. F.; Winpenny, R. E. P. *Nat. Chem.* **2013**, *5*, 673.